From hybrid polariton to dipolariton using non-Hermitian Hamiltonians to handle particle lifetimes

Aurélia Chenu,[1] Shiue-Yuan Shiau,[2] Ching-Hang Chien,[3] and Monique Combescot[4]
[1]*Department of Physics and Materials Science, University of Luxembourg, 1511 Luxembourg, G.D. Luxembourg*
[2]*Physics Division, National Center for Theoretical Sciences, Taipei 10617, Taiwan*
[3]*Research Center for Applied Sciences, Academia Sinica, Taipei 115, Taiwan*
[4]*Sorbonne Université, CNRS, Institut des NanoSciences de Paris, 75005 Paris, France*

(Received 28 October 2021; revised 13 December 2021; accepted 15 December 2021; published 3 January 2022)

We consider photons strongly coupled to the excitonic excitations of a coupled quantum well, in the presence of an electric field. We show how, under a field increase, the hybrid polariton made of a photon coupled to hybrid carriers lying in the two wells transforms into a dipolariton made of a photon coupled to direct and indirect excitons. We also show how the cavity photon lifetime and the coherence time of the carrier wave vectors that we analytically handle through non-hermitian Hamiltonians affect these polaritonic states. While the hybrid polaritons display a spectral singularity where the eigenvalues coalesce, known as an exceptional point, that depends on detuning and lifetimes, we find that the three dipolaritonic states display an anticrossing without exceptional point due to the interaction between photons, direct, and indirect excitons.

DOI: 10.1103/PhysRevB.105.035301

I. INTRODUCTION

Coupled quantum wells (CQWs) provide a unique platform to study the rich quantum properties of excitons [1–6] that have found numerous applications in optoelectronics [7–10]. Of particular interest is a CQW under an electric field perpendicular to the well plane: electrons and holes, which for high-enough field are separated in the two adjacent wells, form spatially indirect excitons, in contrast to direct excitons that are formed from electrons and holes in the same well. The charge separation generates a built-in electric dipole moment that can be controlled by the applied electric field. This was used to control exciton transport in electrostatic [11,12] or optical [13,14] ways and to develop excitonic devices [15]. Such indirect excitons have a long lifetime ranging from 10 ns to 10 μs [10], which exceeds that of direct excitons by orders of magnitude due to the small overlap between electron and hole wave functions that strongly decreases their radiative recombination [16–20]. Thus, they can easily reach thermal equilibrium and allow exploring collective quantum phenomena such as exotic many-body phases [21] and exciton Bose-Einstein condensation [22].

The small overlap between electron and hole wave functions renders indirect excitons quite long-lived, but it also makes them weakly coupled to light. A way to enhance the photon coupling to excitons is to embed the CQW in a microcavity [23]. The resulting exciton-photon particles can be transformed from hybrid polaritons to dipolaritons by applying an external field. In contrast to the hybrid polariton made from cavity photons strongly coupled to hybrid carriers that belong to the two quantum wells, the dipolaritonic modes result from the strong coupling of indirect excitons, direct excitons, and cavity photons. The controllability of the resulting system has inspired new applications such as quantum logic gates [24], optical parametric oscillators [25], tunable single-photon emission [26], and dipolariton Bose-Einstein condensation [27].

In this paper, we consider a CQW in an optical cavity and we study how the cavity photon lifetime and the carrier coherence time affect the dipolariton eigenstates. We wish to recall that, for polaritonic modes to be formed, the coherence time of the exciton wave vector must be long at the exciton-photon coupling scale; otherwise the exciton wave vector $\mathbf{Q}$ would change and the exciton would emit a different photon $\mathbf{Q}' \neq \mathbf{Q}$. The initial $\mathbf{Q}$ photon would thus be lost and the polaritonic mode $\mathbf{Q}$ cannot develop [28].

We here focus on the two limiting cases as follows. (1) In the absence of electric field [see Fig. 1(a)], the electron and hole states result from the hybridization of individual quantum well states, depending on the barrier height and well thickness. The excitons formed from these hybridized states are coupled to photons. The resulting polariton branches then have a lifetime that depends on the photon detuning and the photon and carrier lifetimes. (2) When the electric field is large [see Fig. 1(c)], the electron ground state with energy $\varepsilon_0^{(e)}$ is mainly localized in one well, while the hole ground state with energy $\varepsilon_0^{(h)}$ is mainly in the other well. The first excited states of these carriers, with energies $\varepsilon_1^{(e)}$ and $\varepsilon_1^{(h)}$, are mainly localized the other way around, provided that the electric field is not too large; otherwise the carrier first excited state could be located in the same well as the ground state [29]. The exciton ground state, made of carriers in the $(\varepsilon_0^{(e)}, \varepsilon_0^{(h)})$ levels, is an indirect exciton. The next higher excitonic states, made of carriers in the same well, are direct excitons. The quantum nature of the particles allows them to penetrate the barriers. This induces a small but finite overlap between the electron and hole wave functions. The indirect exciton thus has a small but direct coupling to photons, with no need for any tunneling process that could induce a coupling to photons through direct excitons.

The fact that the photon is coupled to both direct and indirect excitons leads to eigenstates, named dipolaritons, whose

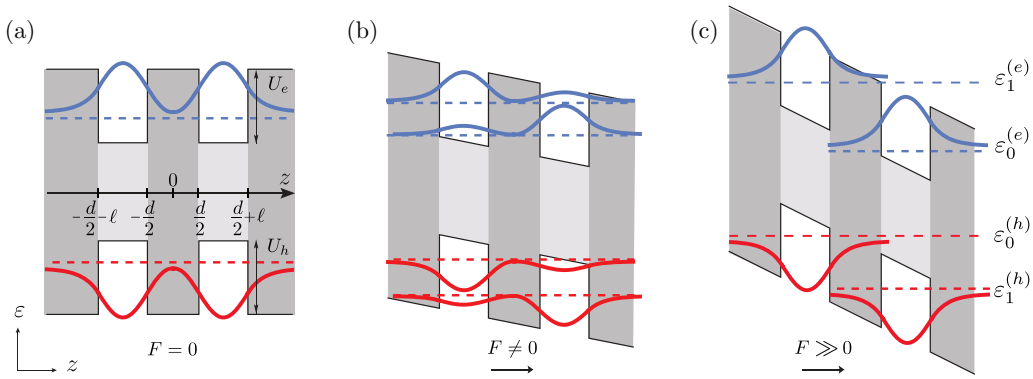

FIG. 1. Schematic representation of carrier energies (dashed lines) and wave functions (solid lines) for electrons (blue) and holes (red) in a coupled quantum well, (a) without or (b), (c) with electric field F. The ground level $\varepsilon_0^{(i)}$ for (a) $F=0$ transforms into two levels under increasing (b), (c) F.

lifetime depends not only on the photon detuning to direct and indirect excitons, but also on the lifetimes of excitons and cavity photons.

The exciton binding energies and the resulting excitonic photoluminescence spectra in a CQW under a static electric field were studied using variational methods [30–32], or by numerically solving the Schrödinger equation of the coupled carriers [18,19]. We here propose an analytical approach to study these energies in which the particle lifetimes is handled through the non-hermitian Hamiltonian approach.

The paper is organized as follows. In Sec. II, we explain how to analytically study cavity photons coupled to quantum well excitons without and with a bias voltage between the two wells. Particular attention is paid to the photon coupling with indirect excitons that was previously understood [23] through electron tunneling between the wells, instead of by just taking into account the existing leakage of the carrier wave functions. We show how to derive the hybrid polariton and dipolariton eigenstates when the particle lifetimes are finite. These lifetimes bring imaginary parts to the particle energies that mathematically lead to non-hermitian Hamiltonians with different bra and ket eigenstates. The diagonal form of the Hamiltonian then appears in terms of creation operators for ket eigenstates and destruction operators for bra eigenstates. Using this non-hermitian formalism, it becomes easy to analytically derive the time evolution of photons coupled to electronic excitations located in two quantum wells, without and with a bias voltage, and to see the transition from hybrid polariton to dipolariton when the detuning and particle lifetimes change. The unbiased case (no field) is presented in Sec. III, with photons coupled to excitons made of electrons and holes in hybridized states. The Hamiltonian then depends on two operators only, the creation operators for photon and hybridized excitons. In Sec. IV, we consider a bias voltage large enough so that the direct excitons, made of electrons and holes in the same quantum well, are well separated in energy from the indirect excitons, made of electrons and holes in different wells. Two kinds of direct excitons and two kinds of indirect excitons *a priori* exist. While the two indirect excitons are well separated in energy so that the one with the highest energy can be eliminated from the problem, the two direct excitons have close energies; they would be equal for identical carrier leakages. It is possible to show that, for equal coupling between photon and direct excitons, one combination of direct excitons is decoupled, while the other gains a $\sqrt{2}$ bosonic enhancement. This leads to a three-body Hamiltonian made of photon, direct, and indirect excitons, that is, a rank-3 eigenvalue equation which can be analytically solved using the Cardan's trick (see the Appendix). The main equations derived in this work are summarized in Table I.

II. GENERAL FORMALISM

A. Semiconductor Hamiltonian

We consider two quantum wells having equal width ℓ separated by a potential barrier with thickness d, as shown in Fig. 1. This CQW structure can be made of two layers of InGaAs materials embedded in a GaAs material. Since the GaAs gap is larger than the InGaAs gap, the electron and hole wave functions along the growth axis z tend to localize inside the InGaAs wells. The carriers move freely in the well planes in the absence of Coulomb interaction.

The semiconductor Hamiltonian for one electron and one hole reduces to

$$H_{\rm eh} = H_e + H_h + V_{\rm eh}. \tag{1}$$

The (H_e, H_h) parts consist of kinetic energies and quantum well potentials for the electron and the hole, with a Coulomb interaction $V_{\rm eh}$ between them.

1. One-body parts

In the presence of external electric field F, the Hamiltonian for the carrier $i=(e,h)$ reads, in the first quantization, as

$$H_i = \frac{\mathbf{p}^2}{2m_i} + U_i(z) \mp |e|Fz, \tag{2}$$

where the minus and plus signs in front of the field energy refers to the electron and hole, respectively. The potential $U_e(z)$ is equal to the difference between the conduction band bottoms of the two semiconductors composing the quantum well, with $U_h(z)$ for the valence band tops. Specifically,

$$U_i(z) = -U_i\,\Theta(z), \tag{3}$$

TABLE I. Summary of the main equations and the parameters used in the paper.

	$F = 0$	Eqs.	$F \gg 0$	Eqs.
Hamiltonian h	$h = \tilde{\omega}\,\alpha^\dagger\alpha + \tilde{\varepsilon}_{0,0} B^\dagger_{0,0} B_{0,0}$		$h \approx \tilde{\omega}\,\alpha^\dagger\alpha + \tilde{\varepsilon}_d\,(B^\dagger_d B_d + D^\dagger_d D_d) + \tilde{\varepsilon}_{id}\,B^\dagger_{id} B_{id}$	
	$+\,(\Omega_{0,0} B^\dagger_{0,0}\alpha + \text{H.c.})$	(36)	$+\,[(\sqrt{2}\,\Omega_d\,B^\dagger_d + \Omega_{id}\,B^\dagger_{id})\alpha + \text{H.c.}]$	(55)
Eigenvectors:				
$(h - \mathcal{E})\lvert P\rangle = 0$	$\lvert P_X\rangle,\ \lvert P_{\text{ph}}\rangle$	(43)	$\lvert P_{id}\rangle,\ \lvert P_d\rangle,\ \lvert P_{\text{ph}}\rangle$	(62–64)
$(h^\dagger - \mathcal{E}^*)\lvert Q\rangle = 0$	$\lvert Q_X\rangle,\ \lvert Q_{\text{ph}}\rangle$	(44)	$\lvert Q_{id}\rangle,\ \lvert Q_d\rangle,\ \lvert Q_{\text{ph}}\rangle$	
Diagonal form	$h = \mathcal{E}_X \frac{P^\dagger_X Q_X}{\langle Q_X \lvert P_X\rangle} + \mathcal{E}_{\text{ph}} \frac{P^\dagger_{\text{ph}} Q_{\text{ph}}}{\langle Q_{\text{ph}} \lvert P_{\text{ph}}\rangle}$	(47)	$h = \mathcal{E}_d \frac{P^\dagger_d Q_d}{\langle Q_d \lvert P_d\rangle} + \mathcal{E}_{id} \frac{P^\dagger_{id} Q_{id}}{\langle Q_{id} \lvert P_{id}\rangle} + \mathcal{E}_{\text{ph}} \frac{P^\dagger_{\text{ph}} Q_{\text{ph}}}{\langle Q_{\text{ph}} \lvert P_{\text{ph}}\rangle}$	(67)
Eigenenergies $\mathcal{E}$	$\mathcal{E} \equiv \mathcal{E}' + \frac{\tilde{\omega}+\tilde{\varepsilon}_{0,0}}{2}$	(41)	$\mathcal{E} \equiv \mathcal{E}' + \frac{\tilde{\omega}+\tilde{\varepsilon}_{id}+\tilde{\varepsilon}_d}{3}$	(60)
with $\mathcal{E}'$	$\mathcal{E}' = \pm\sqrt{(\delta + i\gamma)^2/4 + \lvert\Omega_{0,0}\rvert^2}$	(53)	$\mathcal{E}'^{(n)} = \sum_{s=\pm} e^{is\varphi_n}[\frac{z_3}{2} + s\sqrt{(\frac{z_3}{2})^2 + (\frac{z_2}{3})^3}]^{1/3}$	(71)
Parameters	$\tilde{\omega} = \omega - i\gamma_{\text{ph}};\quad \tilde{\varepsilon}_{0,0} = \varepsilon_{0,0} - i\gamma_X$	(37–38)	$\tilde{\omega} = \omega - i\gamma_{\text{ph}};\quad \tilde{\varepsilon}_d = \varepsilon_{0,1} - i\gamma_X;\quad \tilde{\varepsilon}_{id} = \varepsilon_{0,0} - i\gamma_X$	(56–57)
	$\delta = \omega - \varepsilon_{0,0};\quad \gamma = \gamma_X - \gamma_{\text{ph}}$	(51)	$\delta = \omega - \varepsilon_{id};\quad \delta_X - \varepsilon_d - \varepsilon_{id};\quad \gamma = \gamma_X - \gamma_{\text{ph}}$	(73)
	$\tilde{\omega}' = \tilde{\omega} - (\tilde{\omega} + \tilde{\varepsilon}_{0,0})/2$		$\{\tilde{\omega}'_{id}, \tilde{\omega}'_d, \tilde{\omega}'\} = \{\tilde{\varepsilon}_{id}, \tilde{\varepsilon}_d, \tilde{\omega}\} - (\tilde{\omega} + \tilde{\varepsilon}_{id} + \tilde{\varepsilon}_d)/3$	(74)

with $\Theta(z) = 1$ inside the wells $d/2 < |z| < \ell + d/2$ and $\Theta(z) = 0$ outside (see Fig. 1).

By writing $\mathbf{p}^2$ as $p_z^2 + \mathbf{p}_\parallel^2$, we can separate the electron Hamiltonian H_e into a part $\mathbf{p}_\parallel^2/2m_e$ that describes the free motion in the well plane, and a part that depends on z

$$h_{z,e} = \frac{p_z^2}{2m_e} - U_e\,\Theta(z) - eFz. \tag{4}$$

The wave function of the H_e eigenstate, solution of $(H_e - \varepsilon^{(e)}_{n_e,\mathbf{k}_\parallel})|n_e^{(e)}, \mathbf{k}_\parallel\rangle = 0$, then splits as

$$\langle \mathbf{r} | n_e^{(e)}, \mathbf{k}_\parallel\rangle = \langle z | n_e^{(e)}\rangle \langle \mathbf{r}_\parallel | \mathbf{k}_\parallel\rangle = \phi^{(e)}_{n_e}(z)\,\frac{e^{i\mathbf{k}_\parallel\cdot\mathbf{r}_\parallel}}{L}, \tag{5}$$

where L^2 is the well area, in the direction orthogonal to z, while $\phi^{(e)}_{n_e}(z)$ is the wave function of the $h_{z,e}$ eigenstate $|n_e^{(e)}\rangle$

$$0 = \big(h_{z,e} - \varepsilon^{(e)}_{n_e}\big)\big|n_e^{(e)}\big\rangle, \tag{6}$$

and similarly for the holes.

Let $a^\dagger_{n_e,\mathbf{k}_\parallel}$ and $b^\dagger_{n_h,\mathbf{k}_\parallel}$ be the creation operators of the electron and hole states

$$a^\dagger_{n_e,\mathbf{k}_\parallel}|v\rangle = \big|n_e^{(e)}, \mathbf{k}_\parallel\big\rangle, \tag{7a}$$

$$b^\dagger_{n_h,\mathbf{k}_\parallel}|v\rangle = \big|n_h^{(h)}, \mathbf{k}_\parallel\big\rangle, \tag{7b}$$

with $|v\rangle$ denoting the vacuum state. The one-body part of the electron-hole Hamiltonian (1) then reads in terms of electron and hole operators as

$$H_e + H_h \simeq \sum_{n_e=(0,1)} \sum_{\mathbf{k}_\parallel} \big(\varepsilon^{(e)}_{n_e} + \varepsilon^{(e)}_{\mathbf{k}_\parallel}\big) a^\dagger_{n_e,\mathbf{k}_\parallel} a_{n_e,\mathbf{k}_\parallel} + \sum_{n_h=(0,1)} \sum_{\mathbf{k}_\parallel} \big(\varepsilon^{(h)}_{n_h} + \varepsilon^{(h)}_{\mathbf{k}_\parallel}\big) b^\dagger_{n_h,\mathbf{k}_\parallel} b_{n_h,\mathbf{k}_\parallel}, \tag{8}$$

with $\varepsilon^{(e,h)}_{\mathbf{k}_\parallel} = \hbar^2\mathbf{k}_\parallel^2/2m_{e,h}$.

The $\varepsilon^{(i)}_{n_i}$ energies depend on the electric field F. The carrier ground level $n_i^{(i)} = 0$ for $F = 0$ transforms under increasing F into a ground and an excited level, denoted as $|0^{(i)}\rangle$ and $|1^{(i)}\rangle$. For small F, the carrier wave functions are hybridized over the two wells [see Fig. 1(b)], while for large F they are mainly localized in a single well when the barrier potential is large enough [see Fig. 1(c)]. For small or large F, direct electron-hole pairs have a far larger wave-function overlap than indirect pairs, which makes them more coupled to photons. As shown below, their large coupling has a significant consequence on the effective coupling between photons and indirect pairs. This is why direct pairs have to be taken into account in the construction of the polaritonic states, although their energy is higher than for indirect pairs. By contrast, the other indirect pairs made of electron with energy $\varepsilon_1^{(e)}$ and hole with energy $\varepsilon_1^{(h)}$ have a much higher energy and thus can be neglected.

2. *Two-body interaction*

The Coulomb attraction between one electron and one hole reads in the first quantization as

$$V_{\text{eh}} = -\frac{e^2}{\epsilon_{\text{sc}}|\mathbf{r}_e - \mathbf{r}_h|}, \tag{9}$$

where ϵ_{sc} is the semiconductor dielectric constant. In the second quantization, V_{eh} appears in terms of the electron and holes operators as

$$V_{\text{eh}} \simeq -\sum_{n'_e,n'_h} \sum_{n_e,n_h} \sum_{\mathbf{k}_\parallel,\mathbf{k}'_\parallel} \sum_{\mathbf{q}_\parallel} \mathcal{V}\begin{pmatrix} n'_e,\mathbf{k}_\parallel+\mathbf{q}_\parallel & n_e,\mathbf{k}_\parallel \\ n'_h,\mathbf{k}'_\parallel-\mathbf{q}_\parallel & n_h,\mathbf{k}'_\parallel \end{pmatrix} \times b^\dagger_{n'_h,\mathbf{k}'_\parallel-\mathbf{q}_\parallel} a^\dagger_{n'_e,\mathbf{k}_\parallel+\mathbf{q}_\parallel} a_{n_e,\mathbf{k}_\parallel} b_{n_h,\mathbf{k}'_\parallel}. \tag{10}$$

According to the second quantization procedure [33], the prefactor of this two-body operator is given by

$$\mathcal{V}\begin{pmatrix} n'_e,\mathbf{k}_\parallel+\mathbf{q}_\parallel & n_e,\mathbf{k}_\parallel \\ n'_h,\mathbf{k}'_\parallel-\mathbf{q}_\parallel & n_h,\mathbf{k}'_\parallel \end{pmatrix} = \int d\mathbf{r}_e \int d\mathbf{r}_h \frac{e^2}{\epsilon_{\text{sc}}|\mathbf{r}_e - \mathbf{r}_h|} \left(\phi^{(e)}_{n'_e}(z_e)\frac{e^{i(\mathbf{k}_\parallel+\mathbf{q}_\parallel)\cdot\mathbf{r}_{e\parallel}}}{L}\right)^* \times \left(\phi^{(h)}_{n'_h}(z_h)\frac{e^{i(\mathbf{k}'_\parallel-\mathbf{q}_\parallel)\cdot\mathbf{r}_{h\parallel}}}{L}\right)^* \left(\phi^{(e)}_{n_e}(z_e)\frac{e^{i\mathbf{k}_\parallel\cdot\mathbf{r}_{e\parallel}}}{L}\right) \times \left(\phi^{(h)}_{n_h}(z_h)\frac{e^{i\mathbf{k}'_\parallel\cdot\mathbf{r}_{h\parallel}}}{L}\right), \tag{11}$$

with $d\mathbf{r}_i = dz_i\, d\mathbf{r}_{i\parallel}$. After integrating over $(\mathbf{r}_{e\parallel}, \mathbf{r}_{h\parallel})$, we find that this scattering does not depend on $(\mathbf{k}_\parallel, \mathbf{k}'_\parallel)$; it reduces to

$$\mathcal{V}_{\mathbf{q}_\parallel}\left(\begin{smallmatrix} n'_e & n_e \\ n'_h & n_h \end{smallmatrix}\right) = \frac{2\pi e^2}{L^2 \epsilon_{\rm sc} q_\parallel} \iint dz_e dz_h\, e^{-q_\parallel |z_e - z_h|} \times \left(\phi^{(e)}_{n'_e}(z_e)\phi^{(h)}_{n'_h}(z_h)\right)^* \left(\phi^{(e)}_{n_e}(z_e)\phi^{(h)}_{n_h}(z_h)\right), \quad (12)$$

which evidences its dependence on the wave-function overlap between the n_e and n'_e electron states and between the n_h and n'_h hole states. The largest overlaps correspond to $n_e = n'_e$ and $n'_h = n_h$, that is, to Coulomb processes in which the carriers do not change well, which are the ones leading to direct excitons.

3. Exciton states

The last step is to introduce electron-hole pair operators for the physically relevant states.

The creation operator for a free pair made of an electron in the n_e level and a hole in the n_h level, with a center-of-mass wave vector $\mathbf{Q}_\parallel$ and a relative-motion wave vector $\mathbf{k}_\parallel$, reads

$$B^\dagger_{n_e,n_h;\mathbf{Q}_\parallel,\mathbf{k}_\parallel} = a^\dagger_{n_e,\mathbf{k}_\parallel+\mu_e\mathbf{Q}_\parallel} b^\dagger_{n_h,-\mathbf{k}_\parallel+\mu_h\mathbf{Q}_\parallel}, \quad (13)$$

with $\mu_e = 1 - \mu_h = m_e/M_X$ for $M_X = m_e + m_h$. The electron-hole attraction transforms this free pair into a correlated pair, that is, an exciton with a center-of-mass wave vector $\mathbf{Q}_\parallel$ and a relative-motion index ν, its creation operator reading as

$$B^\dagger_{\mathbf{Q}_\parallel,\nu} = \sum_{n_e,n_h} \sum_{\mathbf{k}_\parallel} B^\dagger_{n_e,n_h;\mathbf{Q}_\parallel,\mathbf{k}_\parallel} \langle n_e, n_h; \mathbf{k}_\parallel | \nu \rangle, \quad (14)$$

the exciton energy being equal to $E_{\mathbf{Q}_\parallel,\nu} = \hbar^2 \mathbf{Q}^2_\parallel / 2M_X + \varepsilon_\nu$. The $\langle n_e, n_h; \mathbf{k}_\parallel | \nu \rangle$ prefactor is the solution of the Schrödinger equation

$$0 = \left(\varepsilon^{(e)}_{n_e} + \varepsilon^{(h)}_{n_h} + \frac{\hbar^2 \mathbf{k}^2_\parallel}{2\mu_X} - \varepsilon_\nu\right) \langle n_e, n_h; \mathbf{k}_\parallel | \nu \rangle - \sum_{n'_e,n'_h} \sum_{\mathbf{q}_\parallel} \mathcal{V}_{\mathbf{q}_\parallel}\left(\begin{smallmatrix} n_e & n'_e \\ n_h & n'_h \end{smallmatrix}\right) \langle n'_e, n'_h; \mathbf{k}_\parallel - \mathbf{q}_\parallel | \nu \rangle, \quad (15)$$

where μ_X is the electron-hole reduced mass given by $\mu_X^{-1} = m_e^{-1} + m_h^{-1}$. The exciton relative-motion energy ε_ν depends on the single-particle energies $\varepsilon^{(e)}_{n_e}$ and $\varepsilon^{(h)}_{n_h}$, and the Coulomb scattering $\mathcal{V}_{\mathbf{q}_\parallel}\left(\begin{smallmatrix} n_e & n'_e \\ n_h & n'_h \end{smallmatrix}\right)$; through them, it also depends on the CQW parameters, U_e, U_h, ℓ, and d.

For problems involving one electron-hole pair only, as the present one, we can replace the $H_{\rm eh}$ Hamiltonian by its diagonal form

$$H_{\rm eh} \simeq \sum_{\mathbf{Q}_\parallel} \sum_\nu E_{\mathbf{Q}_\parallel,\nu} B^\dagger_{\mathbf{Q}_\parallel,\nu} B_{\mathbf{Q}_\parallel,\nu}, \quad (16)$$

which is convenient to derive polaritons.

It is important to note that the exciton eigenstates are linear combinations of n_e electrons and n_h holes; the way these particle wave functions are distributed along z in the two wells depends on the electric field. In general, this distribution is nontrivial and can only be numerically obtained. Excitons that are mainly made of electron-hole pairs located in the same well are called direct, while those mainly made of electron-hole pairs located in different wells are called indirect. When the carrier wave functions are extended in the two wells, the excitons are called hybrid.

B. Photon-semiconductor coupling

In this section, we consider a CQW located in a photon cavity. The photon coupling to direct and indirect excitons is controlled by the electric field through the exciton wave functions. We first consider photon coupling to a bulk exciton and then turn to a CQW exciton to better catch the consequences of the well confinement.

1. Bulk

In three dimensions, a photon with wave vector $\mathbf{Q}$ and creation operator $\alpha^\dagger_{\mathbf{Q}}$ is coupled to free pairs with center-of-mass wave vector $\mathbf{Q}$ and creation operators

$$B^\dagger_{\mathbf{Q},\mathbf{k}} = a^\dagger_{\mathbf{k}+\mu_e\mathbf{Q}} b^\dagger_{-\mathbf{k}+\mu_h\mathbf{Q}}. \quad (17)$$

The photon-semiconductor interaction then reads

$$V_{\rm ph-sc} = \sum_{\mathbf{Q}} \sum_{\mathbf{k}} \Omega_{\mathbf{Q},\mathbf{k}} B^\dagger_{\mathbf{Q},\mathbf{k}} \alpha_{\mathbf{Q}} + \text{H.c.} \quad (18)$$

The coupling $\Omega_{\mathbf{Q},\mathbf{k}}$ is essentially $\mathbf{k}$-independent for semiconductors having conduction and valence bands with different parities, as the ones we here consider; so, $\Omega_{\mathbf{Q},\mathbf{k}} \sim \Omega_{\mathbf{Q}} \sim \Omega_0$, since the photon wave vector $\mathbf{Q}$ is very small compared to the relevant electron wave vectors.

Bulk excitons $B^\dagger_{\mathbf{Q},\nu}|\upsilon\rangle$ are related to free pairs $B^\dagger_{\mathbf{Q},\mathbf{k}}|\upsilon\rangle$ through

$$B^\dagger_{\mathbf{Q},\nu} = \sum_{\mathbf{k}} B^\dagger_{\mathbf{Q},\mathbf{k}} \langle \mathbf{k} | \nu \rangle, \quad (19a)$$

$$B^\dagger_{\mathbf{Q},\mathbf{k}} = \sum_{\nu} B^\dagger_{\mathbf{Q},\nu} \langle \nu | \mathbf{k} \rangle, \quad (19b)$$

where $\langle \mathbf{k} | \nu \rangle$ is the bulk exciton relative-motion wave function in momentum space. This gives the $V_{\rm ph-sc}$ interaction in terms of excitons as

$$V_{\rm ph-sc} = \Omega_0 \sum_{\mathbf{Q}} \sum_\nu B^\dagger_{\mathbf{Q},\nu} \alpha_{\mathbf{Q}} \sum_{\mathbf{k}} \langle \nu | \mathbf{k} \rangle + \text{H.c.} \quad (20)$$

The sum over $\mathbf{k}$ can be calculated by using $\langle \mathbf{k} | \mathbf{r} \rangle = e^{-i\mathbf{k}\cdot\mathbf{r}}/L^{3/2}$: if we multiply $\sum_{\mathbf{k}} \langle \nu | \mathbf{k} \rangle$ by 1 written as $L^{3/2} \langle \mathbf{k} | \mathbf{r} = 0 \rangle$ and use the $|\mathbf{k}\rangle$ state closure relation, the sum over $\mathbf{k}$ reduces to $L^{3/2} \langle \nu | \mathbf{r} = 0 \rangle$. So the photon-semiconductor interaction ultimately appears in terms of three-dimensional (3D) exciton creation operators as

$$V_{\rm ph-sc} = \sum_{\mathbf{Q}} \sum_\nu \Omega_\nu B^\dagger_{\mathbf{Q},\nu} \alpha_{\mathbf{Q}} + \text{H.c.}, \quad (21)$$

with $\Omega_\nu = \Omega_0 L^{3/2} \langle \nu | \mathbf{r} = 0 \rangle$. This, in particular, shows that photons have a larger coupling to low 3D exciton states due to their smaller spatial extension.

2. Coupled quantum wells

The quantum well structure breaks the translational invariance of bulk systems in the z direction. We can derive the

photon coupling from Eq. (18) by first writing $B^\dagger_{\mathbf{Q},\mathbf{k}}$ in terms of the electron and hole states relevant for CQW that are defined in Eq. (7). This is done by writing the free electron creation operator $a^\dagger_{\mathbf{k}}$ in terms of a complete set of $|n_e^{(e)}\rangle$ states along z that are defined in Eq. (6), namely,

$$a^\dagger_{\mathbf{k}} \equiv a^\dagger_{k_z,\mathbf{k}_\parallel} = \sum_{n_e} a^\dagger_{n_e,\mathbf{k}_\parallel} \langle n_e^{(e)}|k_z\rangle, \tag{22}$$

and similarly for the hole. The free pair creation operator $B^\dagger_{\mathbf{Q},\mathbf{k}}$ given in Eq. (17) becomes, in terms of $(a^\dagger_{n_e,\mathbf{k}_\parallel}, b^\dagger_{n_h,\mathbf{k}_\parallel})$ operators,

$$\begin{aligned} B^\dagger_{Q_z,\mathbf{Q}_\parallel;k_z,\mathbf{k}_\parallel} &= a^\dagger_{k_z+\mu_e Q_z,\mathbf{k}_\parallel+\mu_e\mathbf{Q}_\parallel} b^\dagger_{-k_z+\mu_h Q_z,-\mathbf{k}_\parallel+\mu_h\mathbf{Q}_\parallel} \\ &= \sum_{n_e,n_h} \langle n_e^{(e)}|k_z+\mu_e Q_z\rangle\langle n_h^{(h)}|-k_z+\mu_h Q_z\rangle \\ &\quad\times a^\dagger_{n_e,\mathbf{k}_\parallel+\mu_e\mathbf{Q}_\parallel} b^\dagger_{n_h,-\mathbf{k}_\parallel+\mu_h\mathbf{Q}_\parallel}, \end{aligned} \tag{23}$$

$\langle k_z|n_e^{(e)}\rangle$ being the Fourier transform of the $\langle z|n_e^{(e)}\rangle$ electron wave function.

In the following, we will restrict the sum over quantum-well levels to the two lowest states, $|0^{(i)}\rangle$ and $|1^{(i)}\rangle$.

The next step is to transform the free pair creation operator $a^\dagger_{n_e,\mathbf{k}_\parallel+\mu_e\mathbf{Q}_\parallel} b^\dagger_{n_h,-\mathbf{k}_\parallel+\mu_h\mathbf{Q}_\parallel}$ of Eq. (23) into creation operators for excitons with a center-of-mass wave vector $\mathbf{Q}_\parallel$, as in Eq. (14). We get

$$\begin{aligned} B^\dagger_{Q_z,\mathbf{Q}_\parallel;k_z,\mathbf{k}_\parallel} &= \sum_{n_e,n_h} \langle n_e^{(e)}|k_z+\mu_e Q_z\rangle\langle n_h^{(h)}|-k_z+\mu_h Q_z\rangle \\ &\quad\times \sum_\nu B^\dagger_{\mathbf{Q}_\parallel,\nu}\langle \nu|n_e,n_h;\mathbf{k}_\parallel\rangle. \end{aligned} \tag{24}$$

The photon-semiconductor coupling given in Eq. (18) then reads, in terms of CQW excitons, as

$$V_{\text{ph-sc}} = \sum_{Q_z,\mathbf{Q}_\parallel} \sum_\nu \sum_{n_e,n_h} \Omega_{n_e,n_h;\nu} B^\dagger_{\mathbf{Q}_\parallel,\nu} \alpha_{Q_z,\mathbf{Q}_\parallel} + \text{H.c.}, \tag{25}$$

with the prefactor given by

$$\Omega_{n_e,n_h;\nu} = \Omega_0 L\langle \nu|n_e,n_h;\mathbf{r}_\parallel=0\rangle \int_L dz \langle n_e^{(e)}|z\rangle\langle n_h^{(h)}|z\rangle. \tag{26}$$

To obtain this prefactor, we first note that $L\langle \nu|n_e,n_h;\mathbf{r}_\parallel=0\rangle$ is equal to $\sum_{\mathbf{k}_\parallel}\langle \nu|n_e,n_h;\mathbf{k}_\parallel\rangle$, as obtained by using $1 = L\langle \mathbf{k}_\parallel|\mathbf{r}_\parallel=0\rangle$ and the closure relation for the two-dimensional (2D) states $|\mathbf{k}_\parallel\rangle$. Next, to obtain the integral over z, we used the fact that the photon wave vector Q_z is far smaller than the relevant electronic wave vectors; so the sum over k_z reduces to

$$\begin{aligned} &\sum_{k_z} \langle n_e^{(e)}|k_z\rangle\langle n_h^{(h)}|-k_z\rangle \\ &\quad= \int_L dz_e \int_L dz_h \langle n_e^{(e)}|z_e\rangle\langle n_h^{(h)}|z_h\rangle \sum_{k_z}\langle z_e|k_z\rangle\langle z_h|-k_z\rangle. \end{aligned} \tag{27}$$

As $\langle z_h|-k_z\rangle = \langle k_z|z_h\rangle$, the sum over k_z is equal to $\langle z_e|z_h\rangle$; so, we end with

$$\sum_{k_z} \langle n_e^{(e)}|k_z\rangle\langle n_h^{(h)}|-k_z\rangle = \int_L dz \langle n_e^{(e)}|z\rangle\langle n_h^{(h)}|z\rangle, \tag{28}$$

which corresponds to the overlap of the electron and hole wave functions inside the wells.

For indirect excitons, the overlap between the electron and hole localized in different wells is very small, but differs from zero for finite barrier height and thickness because the carrier wave functions do penetrate into the barrier. So indirect excitons are not fully decoupled from photons. As a result, it is not necessary to invoke a tunneling effect between direct and indirect excitons to explain the coupling between photon and indirect exciton. This tunneling actually is another, less direct way to say that carriers leak out of the well.

C. Cavity photons

Due to the carrier confinement in the z direction, bulk photons are poorly coupled to CQW excitons. Confining photons in a cavity selects a set of discrete photon wave vectors along the z direction. This is crucial to possibly form polaritons with CQW excitons. Indeed, as seen from the photon-semiconductor coupling given in Eq. (25), a $\mathbf{Q} = (Q_z, \mathbf{Q}_\parallel)$ photon is coupled to a CQW exciton with the same $\mathbf{Q}_\parallel$ wave vector, whereas the conservation of the Q_z component is lost due to the well confinement. So the exciton can recombine into a photon with different Q_z having essentially the same energy, except if the cavity forces the allowed Q_z components to be different enough in energy.

Let us call $Q_z^{(c)}$ the wave vector of the cavity photon having the lowest energy. For a cavity such that the other possible photon energies are outside the relevant energy range, we can restrict the photon Hamiltonian to

$$H_{\text{ph}} \simeq \sum_{\mathbf{Q}_\parallel} \omega_{\mathbf{Q}_\parallel} \alpha^\dagger_{\mathbf{Q}_\parallel} \alpha_{\mathbf{Q}_\parallel}, \tag{29}$$

with $\alpha^\dagger_{\mathbf{Q}_\parallel} \equiv \alpha^\dagger_{Q_z^{(c)},\mathbf{Q}_\parallel}$ and $\omega_{\mathbf{Q}_\parallel} = v_{\text{ph}}\sqrt{\mathbf{Q}_\parallel^2 + (Q_z^{(c)})^2}$, where v_{ph} is the photon velocity in the material at hand.

D. System Hamiltonian relevant to CQW

By collecting the above results, we can write down the system Hamiltonian for cavity photons interacting with carriers in the CQW as

$$H = H_{\text{ph}} + H_{\text{eh}} + V_{\text{ph-sc}}, \tag{30}$$

with the photon Hamiltonian given in Eq. (29). The other two Hamiltonians depend on the electric field applied to the CQW.

(i) In the absence of electric field ($F = 0$), the exciton ground state is mainly made of electron-hole pairs in their ground level $n_i^{(i)} = 0$ with their wave functions evenly distributed in the two wells [Fig. 1(a)]. The electron-hole Hamiltonian (16) then reduces to

$$H_{\text{eh}} \simeq \sum_{\mathbf{Q}_\parallel} \varepsilon_{0,0;\mathbf{Q}_\parallel} B^\dagger_{0,0;\mathbf{Q}_\parallel} B_{0,0;\mathbf{Q}_\parallel}, \tag{31}$$

with $\varepsilon_{0,0;\mathbf{Q}_\parallel} = \hbar^2\mathbf{Q}_\parallel^2/2M_X + \varepsilon_{\nu_0}$ where ε_{ν_0} is the exciton ground-state energy obtained by restricting (n_e,n_h) states in Eq. (15) to (0,0). These excitons are coupled to cavity photons having the same $\mathbf{Q}_\parallel$ through

$$V_{\text{ph-sc}} \simeq \Omega_{0,0} \sum_{\mathbf{Q}_\parallel} B^\dagger_{0,0;\mathbf{Q}_\parallel} \alpha_{\mathbf{Q}_\parallel} + \text{H.c.} \tag{32}$$

with $\Omega_{0,0} \equiv \Omega_{0,0;\nu_0}$ given in Eq. (26).

The system Hamiltonian then splits as $H = \sum_{\mathbf{Q}_\parallel} h_{\mathbf{Q}_\parallel}$ with $h_{\mathbf{Q}_\parallel}$ given by

$$h_{\mathbf{Q}_\parallel} = \omega_{\mathbf{Q}_\parallel}\alpha^\dagger_{\mathbf{Q}_\parallel}\alpha_{\mathbf{Q}_\parallel} + \varepsilon_{0,0;\mathbf{Q}_\parallel}B^\dagger_{0,0;\mathbf{Q}_\parallel}B_{0,0;\mathbf{Q}_\parallel} + (\Omega_{0,0}B^\dagger_{0,0;\mathbf{Q}_\parallel}\alpha_{\mathbf{Q}_\parallel} + \text{H.c.}). \tag{33}$$

In the following, we will drop the $\mathbf{Q}_\parallel$ index to simplify the notation, with $h_{\mathbf{Q}_\parallel}$ now written as

$$h = \omega\alpha^\dagger\alpha + \varepsilon_{0,0}B^\dagger_{0,0}B_{0,0} + (\Omega_{0,0}B^\dagger_{0,0}\alpha + \text{H.c.}). \tag{34}$$

(ii) When the electric field is large, it is necessary to include both direct and indirect excitons into the problem. The Hamiltonian H also splits as a sum of $h_{\mathbf{Q}_\parallel}$ Hamiltonians, which reads, if we again drop the $\mathbf{Q}_\parallel$ index, as

$$h = \omega\alpha^\dagger\alpha + \sum_{(n_e,n_h)=(0,1)} \varepsilon_{n_e,n_h}B^\dagger_{n_e,n_h}B_{n_e,n_h} + \sum_{(n_e,n_h)=(0,1)} \left(\Omega_{n_e,n_h}B^\dagger_{n_e,n_h}\alpha + \text{H.c.}\right). \tag{35}$$

As schematically shown in Fig. 1(c), the energies of the two direct excitons, $\varepsilon_{0,1}$ and $\varepsilon_{1,0}$, are very close and higher than the $\varepsilon_{0,0}$ energy of the indirect exciton. By contrast, the energy $\varepsilon_{1,1}$ of the other indirect exciton is much higher than the ones of the other three species of excitons. This is why, in the following, we will drop this (1,1) indirect exciton from the h Hamiltonian. Moreover, although the carriers leak out of the well not exactly in the same way, we will for simplicity take $\varepsilon_{0,1} \simeq \varepsilon_{1,0}$ and $\Omega_{0,1} \simeq \Omega_{1,0}$, the photon coupling to direct excitons being much larger than the $\Omega_{0,0}$ coupling to the indirect exciton having the lowest energy.

E. Finite lifetimes

The main purpose of this work is to study the effect of finite lifetimes on the coupled photon-CQW system. A mathematically simple and physically intuitive way to include them into the problem is to add an imaginary part to the exciton energies, that is, to replace ε_{n_e,n_h} by $\tilde{\varepsilon}_{n_e,n_h} = \varepsilon_{n_e,n_h} - i\gamma_X$, where γ_X denotes the inverse lifetime induced by nonradiative mechanisms that weakly depend on the well level. Indeed, the physical processes responsible for the lifetime we here consider, better called "coherence time," are the ones that cause a change in the exciton center-of-mass wave vector, these processes being the same in the two wells. We also include the lifetime of the cavity photon induced by mirror imperfections, through replacing ω by $\tilde{\omega} = \omega - i\gamma_{\text{ph}}$.

The imaginary parts representing these lifetimes render the system Hamiltonian non-hermitian. In the next sections, we show how this can be analytically handled.

III. ZERO ELECTRIC FIELD: HYBRID POLARITON

In the absence of electric field [Fig. 1(a)], the relevant excitons are hybrid excitons with carriers lying in the two wells. Including their lifetimes transforms the Hamiltonian (34) into

$$h = \tilde{\omega}\,\alpha^\dagger\alpha + \tilde{\varepsilon}_{0,0}B^\dagger_{0,0}B_{0,0} + (\Omega_{0,0}B^\dagger_{0,0}\alpha + \text{H.c.}), \tag{36}$$

with

$$\tilde{\omega} = \omega - i\gamma_{\text{ph}}, \tag{37}$$

$$\tilde{\varepsilon}_{0,0} = \varepsilon_{0,0} - i\gamma_X. \tag{38}$$

1. Hybrid polariton state and energy

Due to the particle lifetimes, h differs from $h^\dagger$; so these two operators have different eigenstates. Moreover, since h is not hermitian, its eigenstates are not orthogonal, and their energies are not necessarily real.

Let us look for the h eigenstates

$$0 = (h - \mathcal{E})|P\rangle \tag{39}$$

as a linear combination of exciton state $|X\rangle = B^\dagger_{0,0}|v\rangle$ and photon state $|\alpha\rangle = \alpha^\dagger|v\rangle$, namely, $|P\rangle = x|X\rangle + y|\alpha\rangle$. The eigenstate equation (39) for the hybrid polariton made of a photon coupled to a hybrid exciton lying in the two wells leads to

$$0 = [x(\tilde{\varepsilon}_{0,0} - \mathcal{E}) + y\Omega_{0,0}]|X\rangle + [y(\tilde{\omega} - \mathcal{E}) + x\Omega^*_{0,0}]|\alpha\rangle. \tag{40}$$

Its projection over $\langle X|$ and $\langle\alpha|$ gives two coupled equations for (x, y), which have a nonzero solution provided that their determinant is equal to zero. For

$$\mathcal{E} \equiv \mathcal{E}' + \frac{\tilde{\omega} + \tilde{\varepsilon}_{0,0}}{2}, \tag{41}$$

this determinant appears as

$$0 = \begin{vmatrix} -\tilde{\omega}' - \mathcal{E}' & \Omega_{0,0} \\ \Omega^*_{0,0} & \tilde{\omega}' - \mathcal{E}' \end{vmatrix} = \mathcal{E}'^2 - \tilde{\omega}'^2 - |\Omega_{0,0}|^2 \tag{42}$$

for $\tilde{\omega} - \mathcal{E} \equiv \tilde{\omega}' - \mathcal{E}'$. The hybrid polariton energies $\mathcal{E}$ follow from the two solutions of this equation. Let us call $\mathcal{E}_X$ the solution that goes to $\tilde{\varepsilon}_{0,0}$ and $\mathcal{E}_{\text{ph}}$ the solution that goes to $\tilde{\omega}$, when the coupling $\Omega_{0,0}$ goes to zero. The associated (unnormalized) eigenstates are given by

$$|P_X\rangle = |X\rangle + \frac{\Omega^*_{0,0}}{\mathcal{E}_X - \tilde{\omega}}|\alpha\rangle, \tag{43a}$$

$$|P_{\text{ph}}\rangle = |\alpha\rangle + \frac{\Omega_{0,0}}{\mathcal{E}_{\text{ph}} - \tilde{\varepsilon}_{0,0}}|X\rangle. \tag{43b}$$

Since h is non-hermitian, $h \neq h^\dagger$, the $h^\dagger$ eigenstates, that differ from the h eigenstates, also play a role in the problem. The same derivation shows that the $h^\dagger$ eigenstates simply read as the h eigenstates with $(\mathcal{E}, \tilde{\omega}, \tilde{\varepsilon}_{0,0})$ replaced by $(\mathcal{E}^*, \tilde{\omega}^*, \tilde{\varepsilon}^*_{0,0})$: they read

$$|Q_X\rangle = |X\rangle + \frac{\Omega^*_{0,0}}{\mathcal{E}^*_X - \tilde{\omega}^*}|\alpha\rangle, \tag{44a}$$

$$|Q_{\text{ph}}\rangle = |\alpha\rangle + \frac{\Omega_{0,0}}{\mathcal{E}^*_{\text{ph}} - \tilde{\varepsilon}^*_{0,0}}|X\rangle. \tag{44b}$$

Note that $\langle Q|P\rangle \neq 0$ for $(\gamma_{\text{ph}}, \gamma_X) \neq 0$, while $|Q\rangle = |P\rangle$ for $(\gamma_{\text{ph}}, \gamma_X) = 0$, as expected.

To go further, we introduce the polariton operators associated with the h and $h^\dagger$ eigenstates $|P_X\rangle = P^\dagger_X|v\rangle$ and $|Q_X\rangle = Q^\dagger_X|v\rangle$, and similarly for $P^\dagger_{\text{ph}}$ and $Q^\dagger_{\text{ph}}$. Using Eqs. (43a) and

(44a), these operators that read

$$P_X^\dagger = B_{0,0}^\dagger + \frac{\Omega_{0,0}^*}{\mathcal{E}_X - \tilde{\omega}}\alpha^\dagger, \quad P_{\rm ph}^\dagger = \alpha^\dagger + \frac{\Omega_{0,0}}{\mathcal{E}_{\rm ph} - \tilde{\varepsilon}_{0,0}} B_{0,0}^\dagger,$$

$$Q_X^\dagger = B_{0,0}^\dagger + \frac{\Omega_{0,0}^*}{\mathcal{E}_X^* - \tilde{\omega}^*}\alpha^\dagger, \quad Q_{\rm ph}^\dagger = \alpha^\dagger + \frac{\Omega_{0,0}}{\mathcal{E}_{\rm ph}^* - \tilde{\varepsilon}_{0,0}^*} B_{0,0}^\dagger,$$

fulfill the commutation relations

$$\frac{[Q_X, P_X^\dagger]_-}{\langle Q_X | P_X\rangle} = 1 = \frac{[Q_{\rm ph}, P_{\rm ph}^\dagger]_-}{\langle Q_{\rm ph} | P_{\rm ph}\rangle}, \tag{45}$$

the other commutators being equal to zero. These relations lead us to write the closure relation for hybrid polaritons as

$$\mathbb{I} = \frac{|P_X\rangle\langle Q_X|}{\langle Q_X | P_X\rangle} + \frac{|P_{\rm ph}\rangle\langle Q_{\rm ph}|}{\langle Q_{\rm ph} | P_{\rm ph}\rangle}. \tag{46}$$

The diagonal form of the h Hamiltonian then reads

$$h = \mathcal{E}_X \frac{P_X^\dagger Q_X}{\langle Q_X | P_X\rangle} + \mathcal{E}_{\rm ph} \frac{P_{\rm ph}^\dagger Q_{\rm ph}}{\langle Q_{\rm ph} | P_{\rm ph}\rangle}, \tag{47}$$

as necessary to satisfy $0 = (h - \mathcal{E}_X)|P_X\rangle$ and $0 = (h - \mathcal{E}_{\rm ph})|P_{\rm ph}\rangle$, which is easy to check. The above equations also lead to

$$[h, P_X^\dagger]_- = \mathcal{E}_X P_X^\dagger, \quad [h, P_{\rm ph}^\dagger]_- = \mathcal{E}_{\rm ph} P_{\rm ph}^\dagger. \tag{48}$$

Equations (46) and (47) also provide a compact form for the time evolution operator in the $|\alpha\rangle \otimes |X\rangle$ subspace, namely,

$$e^{-iht} = e^{-i\mathcal{E}_X t} \frac{|P_X\rangle\langle Q_X|}{\langle Q_X | P_X\rangle} + e^{-i\mathcal{E}_{\rm ph} t} \frac{|P_{\rm ph}\rangle\langle Q_{\rm ph}|}{\langle Q_{\rm ph} | P_{\rm ph}\rangle}. \tag{49}$$

2. *Hybrid polariton lifetimes*

The finite lifetimes of the exciton and cavity photon are inherited by the hybrid polariton through the imaginary part of its eigenvalue given in Eqs. (41) and (42). By writing

$$\tilde{\omega} - \tilde{\varepsilon}_{0,0} = \delta + i\gamma, \tag{50}$$

where δ is the photon detuning and γ is the difference between the exciton and photon inverse lifetimes

$$\delta = \omega - \varepsilon_{0,0}, \quad \gamma = \gamma_X - \gamma_{\rm ph}, \tag{51}$$

we can deduce how the photon-exciton interaction couples the two particle lifetimes to the detuning. Let us study this tricky coupling in more detail.

(1) In the absence of a photon-exciton interaction ($\Omega_{0,0} = 0$), Eqs. (41) and (42) give $\mathcal{E}' = \pm(\tilde{\omega} - \tilde{\varepsilon}_{0,0})/2$, that is, $\mathcal{E}_X = \tilde{\varepsilon}_{0,0}$ and $\mathcal{E}_{\rm ph} = \tilde{\omega}$, as expected.

(2) When the photon and the exciton have the same lifetime ($\gamma = 0$), the detuning modifies the energies of the two polariton branches, but their lifetimes stay equal to the common particle lifetime. Indeed, Eqs. (41) and (42) give $\mathcal{E}' = \pm\sqrt{\delta^2/4 + |\Omega_{0,0}|^2}$ which is real; so the two polariton branches have the lifetime of the particle, regardless of the detuning. For a detuning small compared to the photon-exciton coupling $\mathcal{E}' \simeq \pm|\Omega_{0,0}|$, while for large detuning $\mathcal{E}' \simeq \pm\delta/2$ whatever the coupling, as shown in Fig. 2(a).

(3) At the photon-exciton resonance ($\delta = 0$), the energies and lifetimes of the two polariton branches depend on the photon-exciton coupling since at resonance $\mathcal{E}'$ is equal to $\pm\sqrt{|\Omega_{0,0}|^2 - \gamma^2/4}$. For small coupling, $|\Omega_{0,0}| < |\gamma|/2$, the two solutions $\mathcal{E}' = \pm i\sqrt{\gamma^2/4 - |\Omega_{0,0}|^2}$ are purely imaginary; so the energies of the two polariton branches stay equal to the particle energy. Under a coupling increase, their initially different lifetimes converge to the same value when $|\Omega_{0,0}| = |\gamma|/2$ [see Fig. 2(b)]. This holds until the exceptional point [34,35], at which the two eigenvalues coalesce, while for larger coupling the coalescence is lifted. For large coupling, $|\Omega_{0,0}| > |\gamma|/2$, the two solutions $\mathcal{E}' = \pm\sqrt{|\Omega_{0,0}|^2 - \gamma^2/4}$ are real; so the two polariton energies depend on the coupling but their lifetimes stay equal to the lifetime obtained for $|\Omega_{0,0}| = |\gamma|/2$, that is,

$$\bar{\gamma} = \frac{\gamma_X + \gamma_{\rm ph}}{2}. \tag{52}$$

The fact that the two polariton branches have the same average lifetime indicates that polaritons oscillate between photon and exciton faster then the relaxation of any particle.

These limiting cases help us catch the evolution of the hybrid polariton energies and lifetimes as a function of the photon-exciton coupling. We now consider the general case, that is, the photon and exciton having different energies and different lifetimes. To do it, we go back to Eq. (42); its two solutions read

$$\mathcal{E}' = \pm\sqrt{(\delta + i\gamma)^2/4 + |\Omega_{0,0}|^2}. \tag{53}$$

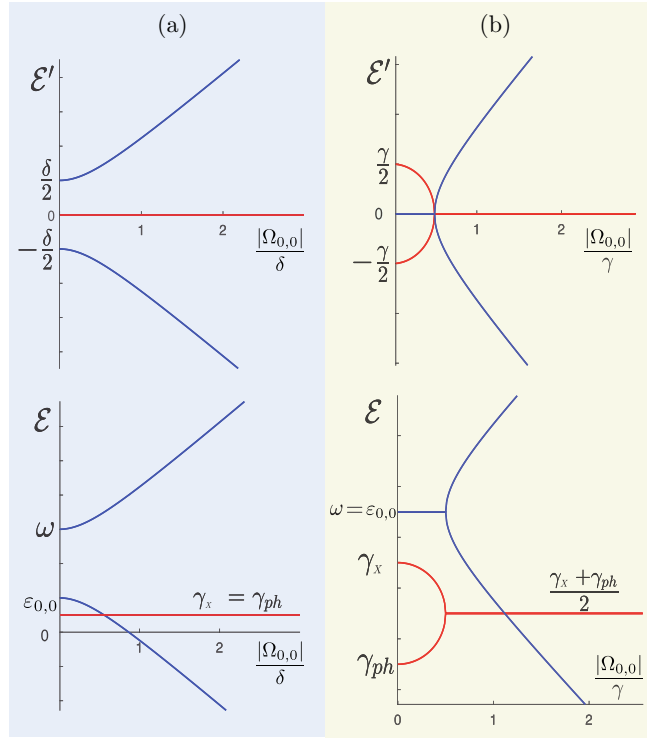

FIG. 2. Hybrid polariton. Dependence of the hybrid polariton energies $(\mathcal{E}', \mathcal{E})$ defined in Eqs. (41) and (53), on the ratio of the photon coupling to hybrid exciton $\Omega_{0,0}$ (a) over the detuning δ when the cavity photon lifetime is equal to the exciton coherence time $0 = \gamma = \gamma_X - \gamma_{\rm ph}$ and (b) over the lifetime difference γ at the photon-exciton resonance $0 = \delta = \omega - \varepsilon_{0,0}$. Real parts (blue) and imaginary parts (red) of $(\mathcal{E}', \mathcal{E})$.

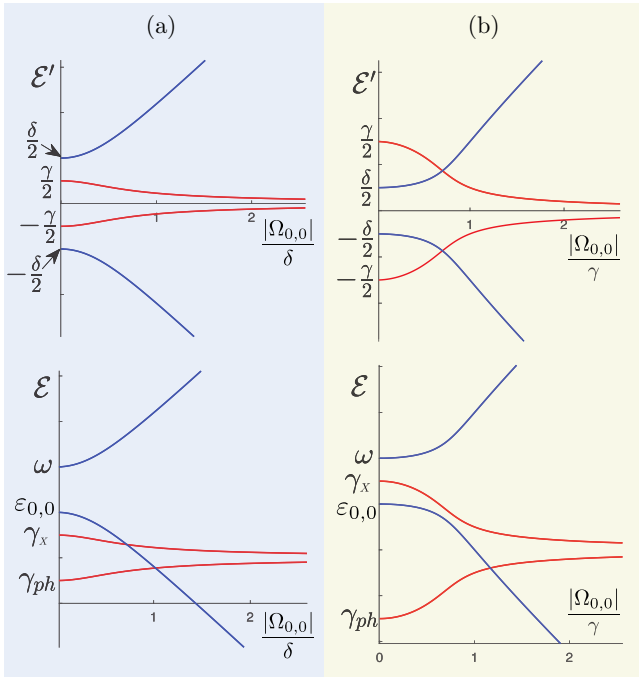

FIG. 3. Hybrid polariton. Same as Fig. 2, for general $\mathcal{E}'$ and $\mathcal{E}$ given in Eq. (53), as a function of the photon-exciton coupling $\Omega_{0,0}$ (a) over the detuning δ for $\delta > \gamma > 0$ and (b) over the lifetime difference γ for $\gamma > \delta > 0$.

These two $\mathcal{E}'$ values evolve from $\pm(\delta + i\gamma)/2$ when $|\Omega_{0,0}| = 0$, to $\pm|\Omega_{0,0}|$ for $|\Omega_{0,0}|$ large compared to $|\delta|$ (see Fig. 3). The energies of the two polariton branches increase with $|\Omega_{0,0}|$, while their lifetimes converge to the average value given in Eq. (52). We note the absence of an exceptional point in this setting.

All this shows that the coupling between the photon and exciton not only changes their energies but also their lifetimes in a tricky way, except when the cavity photon lifetime is equal to the exciton coherence time.

IV. LARGE ELECTRIC FIELD: DIPOLARITON

When the external electric field is large [see Fig. 1(c)], we showed in Eq. (35) that the relevant Hamiltonian consists of a cavity photon coupled to two direct excitons, $B^\dagger_{0,1}$ and $B^\dagger_{1,0}$ with energy $\varepsilon_d \equiv \varepsilon_{0,1} \simeq \varepsilon_{1,0}$, and to a ground-state exciton with energy $\varepsilon_{id} \equiv \varepsilon_{0,0}$, which is an indirect exciton $B^\dagger_{id}$, its electron and hole being in their ground level localized in different wells. We now add the particle lifetimes. By introducing the two linear combinations of direct excitons that are normalized and commute

$$B^\dagger_d = \frac{B^\dagger_{0,1} + B^\dagger_{1,0}}{\sqrt{2}}, \quad D^\dagger_d = \frac{B^\dagger_{0,1} - B^\dagger_{1,0}}{\sqrt{2}}, \tag{54}$$

the h Hamiltonian appears, after dropping the (1,1) indirect exciton, as

$$h \approx \tilde{\omega}\,\alpha^\dagger\alpha + \tilde{\varepsilon}_d\,(B^\dagger_d B_d + D^\dagger_d D_d) + \tilde{\varepsilon}_{id}\,B^\dagger_{id}B_{id} + [(\sqrt{2}\,\Omega_d\,B^\dagger_d + \Omega_{id}\,B^\dagger_{id})\alpha + \text{H.c.}], \tag{55}$$

with the couplings given by $\Omega_d \equiv \Omega_{0,1} \simeq \Omega_{1,0}$ and $\Omega_{id} \equiv \Omega_{0,0}$, while the energies are given by

$$\tilde{\varepsilon}_d \equiv \varepsilon_{0,1} - i\gamma_X = \tilde{\varepsilon}_{0,1} \simeq \tilde{\varepsilon}_{1,0}, \tag{56}$$

$$\tilde{\varepsilon}_{id} \equiv \varepsilon_{0,0} - i\gamma_X. \tag{57}$$

Note the $\sqrt{2}$ enhancement factor that appears in the photon coupling to the $B^\dagger_d$ direct exciton combination. We also note that the $D^\dagger_d$ exciton is not coupled to the cavity photon; so in the following, we will drop it from the h Hamiltonian given in Eq. (55).

A. Dipolariton eigenstates

We proceed as we did for zero electric field. We first look for the h eigenstates $0 = (h - \mathcal{E})|P\rangle$ as a linear combination of indirect exciton $|\text{IX}\rangle = B^\dagger_{id}|v\rangle$, direct exciton $|\text{DX}\rangle = B^\dagger_d|v\rangle$, and cavity photon $|\alpha\rangle = \alpha^\dagger|v\rangle$, namely,

$$|P\rangle = x_{id}|\text{IX}\rangle + x_d|\text{DX}\rangle + y|\alpha\rangle. \tag{58}$$

The equation for the dipolariton eigenstates then reads

$$0 = (x_{id}(\tilde{\varepsilon}_{id} - \mathcal{E}) + y\Omega_{id})|\text{IX}\rangle + (x_d(\tilde{\varepsilon}_d - \mathcal{E}) + \sqrt{2}y\Omega_d)|\text{DX}\rangle + (y(\tilde{\omega} - \mathcal{E}) + x_{id}\Omega^*_{id} + \sqrt{2}x_d\Omega^*_d)|\alpha\rangle. \tag{59}$$

Its projection over $\langle\text{DX}|$, $\langle\text{IX}|$, and $\langle\alpha|$ gives three coupled equations for (x_{id}, x_d, y), which have a nonzero solution provided that their determinant is equal to zero. In terms of

$$\mathcal{E} \equiv \mathcal{E}' + \frac{\tilde{\omega} + \tilde{\varepsilon}_{id} + \tilde{\varepsilon}_d}{3}, \tag{60}$$

this determinant appears as

$$0 = \begin{vmatrix} \tilde{\omega}'_{id} - \mathcal{E}' & 0 & \Omega_{id} \\ 0 & \tilde{\omega}'_d - \mathcal{E}' & \sqrt{2}\,\Omega_d \\ \Omega^*_{id} & \sqrt{2}\,\Omega^*_d & \tilde{\omega}' - \mathcal{E}' \end{vmatrix}, \tag{61}$$

with $\tilde{\omega} - \mathcal{E} \equiv \tilde{\omega}' - \mathcal{E}'$; and similarly for $(\tilde{\omega}'_{id}, \tilde{\omega}'_d)$.

Let us call $\mathcal{E}_{\text{ph}}$ the eigenvalue that tends to $\tilde{\omega}$ when the photon-exciton couplings go to zero, and similarly for $(\mathcal{E}_{id}, \mathcal{E}_d)$. The associated (unnormalized) eigenstates are given by

$$|P_{id}\rangle = |\text{IX}\rangle + \frac{\Omega^*_{id}}{(\mathcal{E}_{id} - \tilde{\varepsilon}_d)(\mathcal{E}_{id} - \tilde{\omega}) - 2|\Omega_d|^2} \times [\sqrt{2}\Omega_d|\text{DX}\rangle + (\mathcal{E}_{id} - \tilde{\varepsilon}_d)|\alpha\rangle], \tag{62}$$

for the indirect-exciton-like branch

$$|P_d\rangle = |\text{DX}\rangle + \frac{\sqrt{2}\Omega^*_d}{(\mathcal{E}_d - \tilde{\varepsilon}_{id})(\mathcal{E}_d - \tilde{\omega}) - |\Omega_{id}|^2} \times [\Omega_{id}|\text{IX}\rangle + (\mathcal{E}_d - \tilde{\varepsilon}_{id})|\alpha\rangle], \tag{63}$$

for the direct-exciton-like branch, and

$$|P_{\text{ph}}\rangle = |\alpha\rangle + \frac{\Omega_{id}}{\mathcal{E}_{\text{ph}} - \tilde{\varepsilon}_{id}}|\text{IX}\rangle + \frac{\sqrt{2}\Omega_d}{\mathcal{E}_{\text{ph}} - \tilde{\varepsilon}_d}|\text{DX}\rangle \tag{64}$$

for the photon-like branch.

To get the $h^\dagger$ eigenstates $0 = (h^\dagger - \mathcal{E}^*)|Q\rangle$ we again have to replace $\mathcal{E}$ by $\mathcal{E}^*$, the $|Q\rangle$ eigenstates being obtained from the $|P\rangle$ eigenstates by changing $(\tilde{\omega}, \tilde{\varepsilon}_d, \tilde{\varepsilon}_{id})$ into $(\tilde{\omega}^*, \tilde{\varepsilon}^*_d, \tilde{\varepsilon}^*_{id})$.

To go further, we introduce the creation operators for the h and $h^\dagger$ eigenstates $|P\rangle = P^\dagger|v\rangle$ and $|Q\rangle = Q^\dagger|v\rangle$. These operators fulfill

$$1 = \frac{[Q_d, P_d^\dagger]_-}{\langle Q_d|P_d\rangle} = \frac{[Q_{id}, P_{id}^\dagger]_-}{\langle Q_{id}|P_{id}\rangle} = \frac{[Q_{\rm ph}, P_{\rm ph}^\dagger]_-}{\langle Q_{\rm ph}|P_{\rm ph}\rangle}, \tag{65}$$

the other commutators being equal to zero. These relations lead to the following closure relation:

$$\mathbb{I} = \frac{|P_d\rangle\langle Q_d|}{\langle Q_d|P_d\rangle} + \frac{|P_{id}\rangle\langle Q_{id}|}{\langle Q_{id}|P_{id}\rangle} + \frac{|P_{\rm ph}\rangle\langle Q_{\rm ph}|}{\langle Q_{\rm ph}|P_{\rm ph}\rangle}. \tag{66}$$

The h Hamiltonian takes a diagonal form in terms of these operators

$$h = \mathcal{E}_d \frac{P_d^\dagger Q_d}{\langle Q_d|P_d\rangle} + \mathcal{E}_{id} \frac{P_{id}^\dagger Q_{id}}{\langle Q_{id}|P_{id}\rangle} + \mathcal{E}_{\rm ph} \frac{P_{\rm ph}^\dagger Q_{\rm ph}}{\langle Q_{\rm ph}|P_{\rm ph}\rangle}, \tag{67}$$

that satisfies $0 = (h - \mathcal{E}_d)|P_d\rangle$, $0 = (h - \mathcal{E}_{id})|P_{id}\rangle$, and $0 = (h - \mathcal{E}_{\rm ph})|P_{\rm ph}\rangle$, as easy to check. Equations (66) and (67) also give the time evolution operator for one photon coupled to direct and indirect excitons in a compact form as

$$e^{-iht} = e^{-i\mathcal{E}_d t} \frac{|P_d\rangle\langle Q_d|}{\langle Q_d|P_d\rangle} + e^{-i\mathcal{E}_{id} t} \frac{|P_{id}\rangle\langle Q_{id}|}{\langle Q_{id}|P_{id}\rangle} + e^{-i\mathcal{E}_{\rm ph} t} \frac{|P_{\rm ph}\rangle\langle Q_{\rm ph}|}{\langle Q_{\rm ph}|P_{\rm ph}\rangle}. \tag{68}$$

B. Dipolariton energies and lifetimes

The eigenvalue equation that follows from the determinant of Eq. (61) reads

$$0 = \mathcal{E}'^3 - z_1\mathcal{E}'^2 + z_2\mathcal{E}' - z_3, \tag{69}$$

with z_i given by

$$\begin{aligned} z_1 &= \tilde\omega'_{id} + \tilde\omega'_d + \tilde\omega' = 0, \\ z_2 &= \tilde\omega'_{id}\tilde\omega'_d + \tilde\omega'_d\tilde\omega' + \tilde\omega'\tilde\omega'_{id} - |\Omega_{id}|^2 - 2|\Omega_d|^2, \\ z_3 &= \tilde\omega'_{id}\tilde\omega'_d\tilde\omega' - 2|\Omega_d|^2\tilde\omega'_{id} - |\Omega_{id}|^2\tilde\omega'_d. \end{aligned} \tag{70}$$

The solution of this third-order equation can be analytically obtained by using the Cardan's trick [36] (see the Appendix). The three solutions read, since $z_1 = 0$,

$$\mathcal{E}'^{(n)} = \sum_{s=\pm} e^{is\varphi_n} \left[\frac{z_3}{2} + s\sqrt{\left(\frac{z_3}{2}\right)^2 + \left(\frac{z_2}{3}\right)^3} \right]^{1/3}, \tag{71}$$

with $\varphi_n = (0, \pm 2\pi/3)$.

C. Physical understanding

Let us now discuss how the couplings of the direct and indirect excitons to the *same* cavity photon modify the particle energies and lifetimes; in particular, how a strong photon coupling to the direct exciton modifies the photon coupling to the indirect exciton when

$$\lambda \equiv \left| \frac{\Omega_{id}}{\sqrt{2}\,\Omega_d} \right| < 1, \tag{72}$$

as obtained for a poor overlap between the carriers making the indirect exciton.

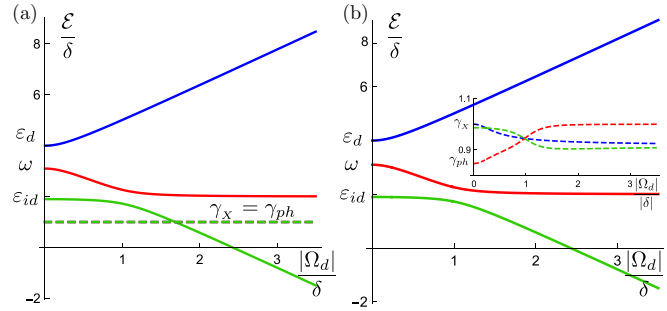

FIG. 4. Dipolariton. Dependence of the dipolariton energies $\mathcal{E}$ on the ratio of the photon coupling to *direct* exciton Ω_d over the detuning with respect to the indirect exciton $\delta = \omega - \varepsilon_{id}$ when the cavity photon and the exciton have (a) the same lifetime $\gamma = 0$ and (b) a lifetime difference $\gamma = \delta/6$. The other parameters are taken as $|\Omega_{id}| = \delta/3$, $\varepsilon_{id} = 2\delta$, $\gamma_X = \delta$, and $\delta_X = \varepsilon_d - \varepsilon_{id} = 2\delta$. The dipolariton has three energy branches given in Eqs. (60), (70), and (71). Their energy real parts are shown as solid lines, while their inverse lifetimes are shown as dashed lines [inset in (b)].

In addition to the ratio λ of the photon couplings to indirect and direct excitons, the other two relevant parameters of the dipolariton problem are the photon detuning δ relative to the indirect exciton ground state and the energy difference δ_X between direct and indirect excitons

$$\delta = \omega - \varepsilon_{id}, \quad \delta_X = \varepsilon_d - \varepsilon_{id}. \tag{73}$$

These three parameters can be experimentally controlled either directly or indirectly. The $\tilde\omega'$ parameters defined in Eq. (61) then read, for $\gamma = \gamma_X - \gamma_{\rm ph}$ as in Eq. (51),

$$\begin{aligned} \tilde\omega'_{id} &= (-\delta_X - \delta - i\gamma)/3, \\ \tilde\omega'_d &= (2\delta_X - \delta - i\gamma)/3, \\ \tilde\omega' &= (2\delta - \delta_X + 2i\gamma)/3. \end{aligned} \tag{74}$$

When the exciton and photon lifetimes are equal, $\gamma = 0$, and when $0 < \delta \ll \delta_X$, that is, when the energy of the direct exciton is much higher than those of the photon and the indirect exciton, the large coupling between the photon and direct exciton coupling Ω_d makes the upper branch of the dipolariton go up to $\mathcal{E}_d \simeq \varepsilon_d + \sqrt{2}\,|\Omega_d|$ and the middle branch go down to $\mathcal{E}_{\rm ph} \simeq \omega - \sqrt{2}\,|\Omega_d|$ until this middle branch anticrosses with the lower branch; the minimum energy splitting between the two is $\simeq 2|\Omega_{id}|$, as obtained by minimizing the energy difference of the two branches with respect to $|\Omega_d|$. Such an anticrossing exists because the lifetimes of the

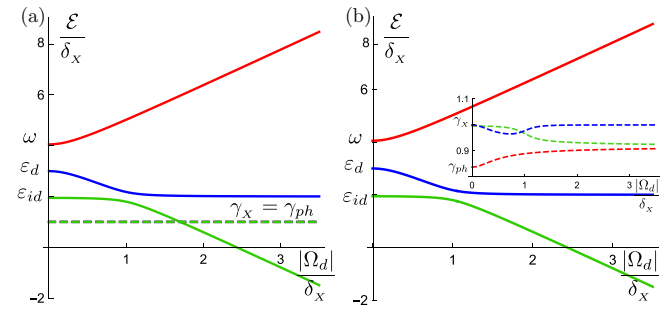

FIG. 5. Dipolariton. Same as Fig. 4 with (δ, δ_X) exchanged.

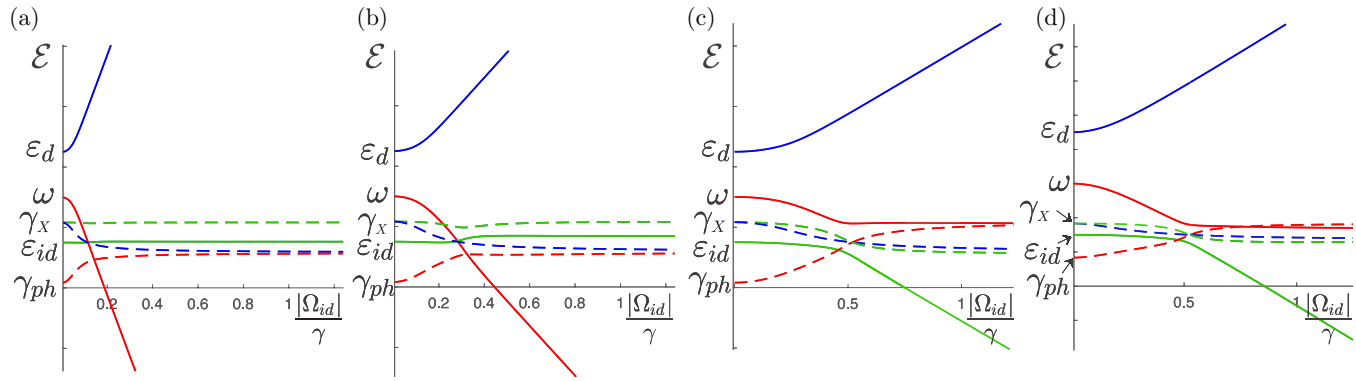

FIG. 6. Dipolariton. Dependence of the dipolariton energies $\mathcal{E}$ on the ratio of the photon coupling to *indirect* exciton $|\Omega_{id}|$ over the lifetime difference $\gamma = \gamma_X - \gamma_{\rm ph}$ for various γ and coupling ratios $\lambda = |\Omega_{id}/\sqrt{2}\,\Omega_d|$. In (a)–(c), γ stays equal to $4\delta/3$ while λ is equal to (0.1; 0.25; 0.5). In (d), λ is equal to 0.25 while $\gamma = 2\delta/3$. All these curves are calculated for $\delta_X = 2\delta$. The dipolariton energy real parts are shown as solid lines, while the dashed lines represent the dipolariton inverse lifetimes.

middle and lower branches are equal. These behaviors are shown in Fig. 4(a) for $\delta_X = 2\delta > 0$ and $|\Omega_{id}| = \delta/3$: as $|\Omega_d|$ increases, an anticrossing occurs between the middle and lower branches, while the middle-branch energy remains flat due to its weak dependence on $|\Omega_d|$. So we end with a hybrid polariton, with the middle branch coupled to the lower branch.

When the exciton and photon lifetimes are equal, $\gamma = 0$, and when $0 < \delta_X \ll \delta$, that is, when the photon energy is much higher than the energies of direct and indirect excitons, the large photon-direct exciton coupling Ω_d makes the upper branch go up to $\mathcal{E}_{\rm ph} \simeq \omega + \sqrt{2}\,|\Omega_d|$, and the middle branch go down to $\mathcal{E}_d \simeq \varepsilon_d - \sqrt{2}\,|\Omega_d|$, until it anticrosses with the lower branch, the minimum energy splitting being

$$\simeq \frac{2|\Omega_{id}|\sqrt{2|\Omega_d|^2 + |\Omega_{id}|^2}}{\delta}, \tag{75}$$

as obtained by minimizing the energy difference of the two branches with respect to $|\Omega_d|$. So we again end with a hybrid polariton with the middle branch coupled to the lower branch, but the effective coupling between the two branches is different from the one for the $0 < \delta \ll \delta_X$ case. The minimum splitting at the anticrossing shown in Fig. 5(a), is smaller than $2|\Omega_{id}|$ as seen from Fig. 4(a).

When the exciton and photon have different lifetimes, $\gamma = \gamma_X - \gamma_{\rm ph} \neq 0$, the lifetimes of the three dipolariton branches depend on the photon-direct exciton coupling $|\Omega_d|$, as seen from the differences between Figs. 4(a) to 5(a) and Figs. 4(b) to 5(b). Surprisingly, for $\gamma = |\Omega_{id}|/2 \neq 0$, the inverse lifetimes of the three dipolariton branches go to a single value as $|\Omega_d|/\delta$ increases [see Fig. 4(b)], while the middle and lower branches anticross with a splitting smaller than the one for $\gamma = 0$. Before this point, the photonic branch has the largest lifetime, while for larger $|\Omega_d|$, this branch has the smallest lifetime, the two inverse excitonic lifetimes converging to a smaller value in the large $|\Omega_d|$ limit. Indeed, for $\delta \ll \delta_X$, the splitting at the anticrossing is approximately equal to $2\sqrt{(1+\delta/\delta_X)|\Omega_{id}|^2 - \gamma^2/4}$. Equal inverse lifetimes mathematically mean that the three $\mathcal{E}'$ solutions of Eq. (69) are real. This provides a tool to mitigate the short nonradiative lifetime of the excitons.

When the upper branch is photon-like, as shown in Fig. 5(b), the middle and lower exciton-like branches anticross; their inverse lifetimes go to a single value at $|\Omega_d| = \delta_X$, while the inverse lifetime of the upper branch, that remains the smallest for all $|\Omega_d|$ values, goes to the lower branch value for large $|\Omega_d|$.

We now turn to the effect of the photon couplings to indirect and direct excitons, through their ratio λ. When λ is small, see Figs. 6(a) and 6(b), the energies of the middle and lower branches can cross because the lifetimes of these two branches are different whatever $|\Omega_{id}|$. The energy and lifetime of the branch that start from the indirect exciton (green curves) remain flat as $|\Omega_{id}|$ increases, which is the signature of indirect exciton being weakly coupled to photon and to direct exciton. This is in contrast to Fig. 4(b) which exhibits an anticrossing: as λ increases, the lower two branches anticross and the lifetimes of the three branches go to the same value, as shown in Fig. 6(c) for $\lambda = 0.5$, which is reminiscent of the results in Fig. 4(b). Note that we can also obtain an anticrossing by decreasing the inverse lifetime difference γ, as can be seen by comparing Fig. 6(b) and 6(d).

V. CONCLUSION

In this work, we studied how cavity photons couple to direct and indirect excitons in a coupled quantum well when the external electric field increases, with a particular focus on the effect of the particle lifetimes. To do so, we first constructed the relevant system Hamiltonians step by step, from scratch. Their diagonal form allowed us to identify the various states that are relevant to the problem at hand. The procedure to derive diagonal Hamiltonian operators can be easily extended to multilevel systems. Then, we showed how, at low electric field, the photon couples to a hybrid exciton made of carriers lying in the two quantum wells, to form a hybrid polariton. By contrast, at large electric field, the photon couples to one indirect exciton and two direct excitons, then forming a dipolariton. By adding the lifetime of the cavity photon and the coherence time of the exciton carriers, we derived the consequences of the carrier relaxation processes and precisely tracked the time evolution of this open quantum system. We were able to do it with the help of non-hermitian

Hamiltonians. By showing how the polariton energies are affected by these lifetimes, our work provides physical insights to possibly identify the parameter regime in which the dipolariton can be created.

ACKNOWLEDGMENTS

We wish to thank François Dubin for initiating this work and for numerous insights.

APPENDIX: RESOLUTION OF EQ. (69)

The analytical solution of Eq. (69) follows from the Cardan's trick [36]: we write $\mathcal{E}'$ as $U + a/U$ and we choose a such that the resulting equation

$$0 = U^3 + \frac{a^3}{U^3} + \left(U + \frac{a}{U}\right)(3a + z_2) - z_3 \tag{A1}$$

has no term in U and $1/U$. This leads to $a = -z_2/3$. The above equation then reduces to $0 = U^6 - z_3 U^3 + a^3$. Its solutions simply read

$$U_\pm^3 = \frac{z_3}{2} \pm \sqrt{\left(\frac{z_3}{2}\right)^2 + \left(\frac{z_2}{3}\right)^3}, \tag{A2}$$

which leads to

$$U_{m,\pm} = e^{im2\pi/3}\left[\frac{z_3}{2} \pm \sqrt{\left(\frac{z_3}{2}\right)^2 + \left(\frac{z_2}{3}\right)^3}\right]^{1/3} \tag{A3}$$

for $m = (0, \pm 1)$. The resulting solutions of Eq. (69) are given by

$$\mathcal{E}'_{m,\pm} = U_{m,\pm} - \frac{z_2/3}{U_{m,\pm}}. \tag{A4}$$

Note that Eq. (A3) seems to give six values while Eq. (70) is a cubic equation with only three solutions. To fix this problem, we note that $U_{m,+}U_{-m,-} = -z_2/3$; so the solutions with a $+$ and $-$ sign in Eq. (A3) are related by $\mathcal{E}'_{m,+} = \mathcal{E}'_{-m,-}$. Consequently, the three solutions of Eq. (69) can be taken either as the three values of $\mathcal{E}'_{m,+}$ or the three values of $\mathcal{E}'_{-m,-}$.

[1] D. A. B. Miller, D. S. Chemla, T. C. Damen, A. C. Gossard, W. Wiegmann, T. H. Wood, and C. A. Burrus, Phys. Rev. B **32**, 1043 (1985).

[2] H. Q. Le, J. J. Zayhowski, and W. D. Goodhue, Appl. Phys. Lett. **50**, 1518 (1987).

[3] L. V. Butov, A. Imamoglu, A. V. Mintsev, K. L. Campman, and A. C. Gossard, Phys. Rev. B **59**, 1625 (1999).

[4] A. V. Larionov, V. B. Timofeev, J. Hvam, and K. Soerensen, J. Exp. Theor. Phys. **90**, 1093 (2000).

[5] L. V. Butov, A. C. Gossard, and D. S. Chemla, Nature (London) **418**, 751 (2002).

[6] M. Combescot, R. Combescot, and F. Dubin, Rep. Prog. Phys. **80**, 066501 (2017).

[7] D. Ahn, IEEE J. Quantum Electron. **25**, 2260 (1989).

[8] Y. Tokuda, K. Kanamoto, and N. Tsukada, Appl. Phys. Lett. **56**, 166 (1990).

[9] A. A. High, A. T. Hammack, L. V. Butov, M. Hanson, and A. C. Gossard, Opt. Lett. **32**, 2466 (2007).

[10] A. A. High, E. E. Novitskaya, L. V. Butov, M. Hanson, and A. C. Gossard, Science **321**, 229 (2008).

[11] A. G. Winbow, J. R. Leonard, M. Remeika, Y. Y. Kuznetsova, A. A. High, A. T. Hammack, L. V. Butov, J. Wilkes, A. A. Guenther, A. L. Ivanov, M. Hanson, and A. C. Gossard, Phys. Rev. Lett. **106**, 196806 (2011).

[12] G. J. Schinner, J. Repp, E. Schubert, A. K. Rai, D. Reuter, A. D. Wieck, A. O. Govorov, A. W. Holleitner, and J. P. Kotthaus, Phys. Rev. Lett. **110**, 127403 (2013).

[13] M. Alloing, A. Lemaître, E. Galopin, and F. Dubin, Sci. Rep. **3**, 1578 (2013).

[14] A. T. Hammack, M. Griswold, L. V. Butov, L. E. Smallwood, A. L. Ivanov, and A. C. Gossard, Phys. Rev. Lett. **96**, 227402 (2006).

[15] P. Andreakou, S. V. Poltavtsev, J. R. Leonard, E. V. Calman, M. Remeika, Y. Y. Kuznetsova, L. V. Butov, J. Wilkes, M. Hanson, and A. C. Gossard, Appl. Phys. Lett. **104**, 091101 (2014).

[16] J. A. Kash, E. E. Mendez, and H. Morkoç, Appl. Phys. Lett. **46**, 173 (1985).

[17] Z. Vörös, R. Balili, D. W. Snoke, L. Pfeiffer, and K. West, Phys. Rev. Lett. **94**, 226401 (2005).

[18] K. Sivalertporn, L. Mouchliadis, A. L. Ivanov, R. Philp, and E. A. Muljarov, Phys. Rev. B **85**, 045207 (2012).

[19] K. Sivalertporn and E. A. Muljarov, Phys. Rev. Lett. **115**, 077401 (2015).

[20] M. Beian, M. Alloing, E. Cambril, C. G. Carbonell, J. Osmond, A. Lemaître, and F. Dubin, Europhys. Lett. **110**, 27001 (2015).

[21] R. Anankine, M. Beian, S. Dang, M. Alloing, E. Cambril, K. Merghem, C. G. Carbonell, A. Lemaître, and F. Dubin, Phys. Rev. Lett. **118**, 127402 (2017).

[22] M. Beian, M. Alloing, R. Anankine, E. Cambril, C. G. Carbonell, A. Lemaître, and F. Dubin, Europhys. Lett. **119**, 37004 (2017).

[23] P. Cristofolini, G. Christmann, S. I. Tsintzos, G. Deligeorgis, G. Konstantinidis, Z. Hatzopoulos, P. G. Savvidis, and J. J. Baumberg, Science **336**, 704 (2012).

[24] O. Kyriienko and T. C. H. Liew, Phys. Rev. B **93**, 035301 (2016).

[25] P. I. Khadzhi and O. F. Vasilieva, JETP Lett. **102**, 581 (2015).

[26] O. Kyriienko, I. A. Shelykh, and T. C. H. Liew, Phys. Rev. A **90**, 033807 (2014).

[27] V. Shahnazaryan, O. Kyriienko, and I. A. Shelykh, Phys. Rev. B **91**, 085302 (2015).

[28] F. Dubin, M. Combescot, and B. Roulet, Europhys. Lett. **69**, 931 (2005).

[29] K. Sivalertporn, Phys. Lett. A **380**, 1990 (2016).

[30] T. Kamizato and M. Matsuura, Phys. Rev. B **40**, 8378 (1989).

[31] M. M. Dignam and J. E. Sipe, Phys. Rev. B **43**, 4084 (1991).

[32] J. Soubusta, R. Grill, P. Hlídek, M. Zvára, L. Smrčka, S. Malzer, W. Geißelbrecht, and G. H. Döhler, Phys. Rev. B **60**, 7740 (1999).

[33] M. Combescot and S.-Y. Shiau, *Excitons and Cooper Pairs* (Oxford University Press, New York, 2016).

[34] T. Kato, *Perturbation Theory for Linear Operators* (Springer-Verlag, Berlin, 1966).

[35] Y. Ashida, Z. Gong, and M. Ueda, Adv. Phys. **69**, 249 (2020).

[36] R. W. D. Nickalls, Math. Gaz. **77**, 354 (1993).